6376 *Macromolecules* **1997,** *30,* 6376−6384

Microscopic Theory for the “Lozenge” Contour Plots in Scattering from Stretched Polymer Networks

D. J. Read* and T. C. B. McLeish

Department of Physics, University of Leeds, IRC in Polymer Science & Technology, Department of Physics, University of Leeds, Leeds, LS2 9JT, U.K.

Received April 24, 1997; Revised Manuscript Received July 7, 1997[⊗]

ABSTRACT: We present a consistent explanation for the appearance of “lozenge” shapes in contour plots of the two-dimensional scattering intensity from stretched polymer networks. We show that lozenge patterns arise as a result of chain material that is not directly deformed by the stretch. This accounts for the lozenges which appear in scattering from pure polymer networks with some labeled chains, which we show explicitly by taking the model of a labeled chain whose midsection is confined to a stretched tube but whose ends are unconstrained. The model produces excellent fits to data. We discuss qualitatively the lozenges which are a precursor to “butterfly” patterns in scattering from networks containing a mobile labeled component. We also show that lozenges cannot consistently be explained by coupling tube constraints to the stretch alone.

1. Introduction

Recently there have been a number of neutron scattering experiments on uniaxially deformed polymer networks and melts. A common observation in these experiments is that contour plots of the two-dimensional scattering intensity take on a diamond or “lozenge” shape. The experiments fall mainly into two categories: for pure networks with dilute labeled chains,[1] the lozenge pattern is permanent and does not relax, but if the labeled species is mobile, the lozenge pattern relaxes and is a precursor to “butterfly” contour patterns.[2,3] In this paper, we demonstrate that the lozenge shape can largely be explained by taking into account those chain sections in the system which are not directly deformed by the stretch. We concentrate mainly on the case of pure networks containing labeled chains, though the concepts are transferable to systems with a mobile species.

In a polymer network, the effect of cross-links and topological entanglements is to localize the network chains in space. Each monomer is confined to a region around its mean position, and deviations from this result in an elastic energy penalty due to the deformation of the surrounding network. The complete “many-chain” description of such effects in networks is a very difficult statistical mechanical problem, and a common approach is to attempt to capture the essential physics by considering the effect of the entire network on individual chains via an “effective field”.

One such approach was used by Edwards and coworkers.[4,5] The effect of the network on a given chain was modeled by placing each monomer on the chain in a harmonic localizing potential. Localizing a chain in this manner leads naturally to the concept of a “tube” because the mean path of the chain is then fixed by the positions of the localizing potentials. The model was used by Warner and Edwards[5] to predict the neutron scattering function for a stretched network in which a fraction of the chains are entirely deuterated. The result was a scattering function with an affine component (related to the mean path) and an isotropic component (related to fluctuations within the tube).

A modified form of the Warner−Edwards result has been used recently by Straube et al.[1,6,7] to interpret a series of experiments on stretched, labeled networks. One experiment[1] involved scattering from networks formed by cross-linking melts which contained a small fraction of deuterated chains. This experiment provided a crucial test for the Warner−Edwards result. It was found that the original Warner−Edwards expression did not consistently fit the neutron scattering patterns obtained. Specifically, the expression does not yield the experimentally observed lozenges. It is clear that, at the very least, some modifications to the original model are necessary.

Straube et al. presented a modified version of the Warner−Edwards result which fitted the data well in two important aspects: (i) the lozenge appearance of the scattering contour plots and (ii) the reproduction of the “isotropy angle”,[8] along which the scattering of the stretched system is identical to that of the undeformed network for all $|\mathbf{q}|$. The modifications were based on the suggestion that, when the chains are entangled, the harmonic localizing potentials in the model couple to the macroscopic strain.[9,10] However, the modifications were empirically introduced at the level of the final result of Warner and Edwards and not at the level of the basic microscopic model. In particular, we believe that one of the modifications introduced is inconsistent with the original Edwards model.

Since the fits obtained by Straube et al. are good, it is necessary to discuss briefly the inconsistencies between their result and the Warner−Edwards model. This is the subject of the first section of this paper. We re-examine the original Warner−Edwards model at the microscopic level and show how coupling the harmonic potentials with the macroscopic strain affects the final result. We seek to clarify the additional assumptions that must be made in order to obtain the result used by Straube et al. We shall find that, if these assumptions are implemented at the fundamental level, it is no longer possible to account for either observation (i) or (ii) above.

In the second section of this paper, we demonstrate that lozenge patterns can easily be obtained by taking into account those chain sections which remain undeformed by the stretch because they possess at least one end unattached to the network.[11] While combinations of stretched and undeformed material have been cited in early discussions of the lozenge pattern,[2] these

---

[⊗] Abstract published in *Advance ACS Abstracts,* September 1, 1997.

S0024-9297(97)00571-8 CCC: $14.00

explanations have relied on a direct link between the mechanisms for “butterfly” and “lozenge” patterns. In contrast, we obtain lozenge patterns independently of the “butterfly” mechanism. We take the specific model of a chain confined to an Edwards tube except that we allow the chain to have isotropic “dangling ends”. Using this model, we are able to obtain excellent fits to experimental data. We are also able to discuss the effect of coupling the tube potential to macroscopic strain with regard to both fitting the data and describing of the experimentally observed isotropy angle. The latter is not found to be a reliable discriminator between models. Finally, we discuss how the concepts of this paper may be transferred to explain the lozenges observed in butterfly pattern experiments.

2. Discussion of Previous Theories

We consider the original system for which the Warner–Edwards theory was derived: a network containing a fraction of completely deuterated chains. It is instructive to rederive the Warner–Edwards expression. Their original calculation[5] made use of the replica field trick to perform the necessary averaging. We have found that, since all the potentials involved are harmonic, it is possible to complete the calculation using Gaussian integrals only and without resorting to the replica method.

2.1. Rederivation of the Warner–Edwards Expression. Consider a labeled Gaussian chain in a network. The position of monomer l on this chain is $\mathbf{r}_l$, and each monomer is coupled by a localizing gaussian potential to fixed points $\mathbf{R}_l$. The total free energy functional for the chain (in units of k_BT) is

$$F_{\mathbf{R}}\{r_{\mu,l}\} = \frac{1}{2}\sum_{\mu,l}\left[\frac{3}{b^2}\left(\frac{\partial r_{\mu,l}}{\partial l}\right)^2 + w^2(r_{\mu,l} - R_{\mu,l})^2\right] \qquad (1)$$

where $r_{\mu,l}$ is the component of $\mathbf{r}_l$ in the Cartesian direction μ ($=x,y,z$). The first term represents the Gaussian chain statistics (b is the step length), and the second term represents the localizing potentials. For now, we assume (following Warner and Edwards) that the strength, w, of these potentials is strain-independent and isotropic.

Since the tube potentials represent the localizing effect of the network, for any given chain they are fixed at the time of formation of the network. For this reason, the $R_{\mu,l}$ must be treated as “quenched” variables, only to be averaged at the end of any calculation. The true “annealed” average for the system is an average over the configurations available to the chain at fixed $R_{\mu,l}$. We denote this average by $\langle ... \rangle_{\mathbf{R}}$, and it is given by an integral over the $r_{\mu,l}$:

$$\langle ... \rangle_{\mathbf{R}} = \int D\{r_{\mu,l}\}\ ...\ A(R_{\mu,l}) \exp(-F_{\mathbf{R}}\ \{r_{\mu,l}\}) \qquad (2)$$

where $A(R_{\mu,l})$ is a normalization factor which depends on the quenched positions of the harmonic potentials.

The averages are most easily performed by considering the normal modes of the chain under the harmonic potentials. These are given by $r_{\mu,p}$, such that

$$r_{\mu,l} = \sum_p r_{\mu,p} \exp(ilp) \qquad (3)$$

In the normal coordinates, the annealed average of eq 2 becomes

$$\langle ... \rangle_{\mathbf{R}} = \int D\{r_{\mu,p}\}\ ...\ A \exp\left[-\frac{N}{2}\sum_{\mu,p} r_{\mu,p}r_{\mu,-\mathrm{p}}w^2\left(1 + \frac{3p^2}{b^2w^2}\right) - 2r_{\mu,p}R_{\mu,-p}w^2 + R_{\mu,p}R_{\mu,-p}w^2\left(1 + \frac{3p^2}{b^2w^2}\right)^{-1}\right] \qquad (4)$$

where the $R_{\mu,-p}$ dependence of the normalization constant A has been accounted for in the exponential. N is the total number of monomers on the chain.

In experiments, the neutron scattering is due to variations in the local density of labeled monomers, given in this model (for the single chain) by

$$\rho(\mathbf{r}) = \sum_l \delta(\mathbf{r} - \mathbf{r}_l) \qquad (5)$$

which has Fourier transform

$$\begin{aligned}\rho_{\mathbf{q}} &= \int d^3\mathbf{r}\rho(\mathbf{r}) \exp(i\mathbf{q}\cdot\mathbf{r}) \\ &= \sum_l \exp(i\mathbf{q}\cdot\mathbf{r}_l) \end{aligned} \qquad (6)$$

and the elastic scattering from a single chain with fixed harmonic potentials is given by $\langle \rho_{\mathbf{q}}\rho_{-\mathbf{q}}\rangle_{\mathbf{R}}$. Since a neutron beam is large enough to sample many labeled chains, it is appropriate to consider the average scattering over the possible configurations of the harmonic potentials. We denote the average over the quenched variables $R_{\mu,p}$ by $\overline{(...)}$, so that

$$\overline{(...)} = \int D\{R_{\mu,p}\}\ ...\ P(R_{\mu,p}) \qquad (7)$$

where $P(R_{\mu,p})$ is the probability distribution for the fixed $R_{\mu,p}$. This is chosen subject to two constraints. First, the $R_{\mu,p}$ must deform affinely with the macroscopic strain. Second, in the unstrained network, the average chain configuration must be Gaussian with step length b. By integrating eq 4 over a general Gaussian distribution of $R_{\mu,p}$, and then insisting on these two constraints, it can easily be shown that the required probability distribution for the $R_{\mu,p}$ is

$$P(R_{\mu,p}) \sim \exp\left[-\frac{N}{2}\sum_{\mu,p} R_{\mu,p}R_{\mu,-p}\frac{3p^2}{{\lambda_\mu}^2b^2}\left(1 + \frac{3p^2}{b^2w^2}\right)^{-1}\right] \qquad (8)$$

where λ_μ is the macroscopic strain ratio in the direction μ, and we have chosen the reference axes such that the strain tensor is diagonalized. Note that the configuration of the $R_{\mu,p}$ differs from that of a Gaussian random walk at small length scales (high p).[9]

To complete the derivation, we perform Gaussian integrals in the quenched and annealed averages to obtain

$$\overline{\langle \rho_{\mathbf{q}}\rho_{-\mathbf{q}}\rangle_{\mathbf{R}}} = \sum_{l,l'} \exp\left[-\frac{1}{2N}\sum_{\mu,p} {q_\mu}^2 \left|e^{ilp} - e^{il'p}\right|^2\left(\frac{{\lambda_\mu}^2b^2}{3p^2} + \frac{(1 - {\lambda_\mu}^2)}{w^2(1+3p^2/b^2w^2)}\right)\right] \qquad (9)$$

The sum over the normal co-ordinates p can be performed by taking the continuous chain limit ($N \to \infty$, such that $Nb^2/6 = {R_g}^2$ is constant) in which case the sum becomes an integral ($1/N\sum_p \to 1/2\pi\int dp$) and we find

$$N^{-2}\overline{\langle\rho_{\mathbf{q}}\rho_{-\mathbf{q}}\rangle_{\mathbf{R}}} = \int_0^1 \mathrm{d}x \int_0^1 \mathrm{d}x' \exp\left[-\sum_\mu Q_\mu^{\,2}\lambda_\mu^{\,2}\left|x-x'\right| + Q_\mu^{\,2}(1-\lambda_\mu^{\,2})\,\frac{d^2}{2\sqrt{6}R_\mathrm{g}^{\,2}}\left(1-\exp\left(-\frac{2\sqrt{6}R_\mathrm{g}^{\,2}|x-x'|}{d^2}\right)\right)\right]$$

The Warner–Edwards Result (10)

We have used the same notation as Straube et al.[1] for consistency: R_g is the radius of gyration of the undeformed chain, $Q_\mu = q_\mu R_\mathrm{g}$ is the normalized wavevector, and $x = l/N$ and $x' = l'/N$ are chain contour length coordinates. The tube diameter d is related to the harmonic potentials w by

$$d^2 = \sqrt{2}b/w \tag{11}$$

The mean-square fluctuation of a monomer about its mean position is proportional to d^2.

Physically, the Warner–Edwards expression (eq 10) indicates a separation of length scales which becomes apparent by examining the term in the exponent:

$$\sum_\mu Q_\mu^{\,2}\lambda_\mu^{\,2}|x-x'| + Q_\mu^{\,2}(1-\lambda_\mu^{\,2})\frac{d^2}{2\sqrt{6}R_\mathrm{g}^{\,2}}\left(1-\exp\left(-\frac{2\sqrt{6}R_\mathrm{g}^{\,2}|x-x'|}{d^2}\right)\right) \tag{12}$$

For monomers separated by many entanglement lengths ($|x-x'| \gg d^2/R_\mathrm{g}^2$) the term $Q_\mu^2\lambda_\mu^2|x-x'|$ dominates. This term is the result obtained by affinely deforming a Gaussian chain. For monomers well within an entanglement length of each other ($|x-x'| \ll d^2/R_\mathrm{g}^2$), the tube potential becomes less important, and the local chain configuration is isotropic. In this limit, the leading order term in the exponent of eq 10 is that of an undeformed chain, $Q_\mu^2|x-x'|$. So, at large length scales, the chain configuration is fixed by the tube and is affinely deformed, but at smaller length scales, the isotropic fluctuations within the tube become important. However, the Warner–Edwards expression does not give the experimentally observed lozenge contour plots.

2.2. Coupling the Tube Constraint to the Macroscopic Strain.

In order to fit their data, Straube et al.[1] proposed that the localizing potentials couple in some way to the macroscopic strain. Such a coupling has been suggested by various authors.[9,10,12] This means using an anisotropic harmonic potential for the part of the free energy functional due to the tube, so that the free energy for the stretched chain becomes

$$F_\mathbf{R}\{r_{\mu,l}\} = \frac{1}{2}\sum_{\mu,l}\left[\frac{3}{b^2}\left(\frac{\partial r_{\mu,l}}{\partial l}\right)^2 + w_\mu^{\,2}(r_{\mu,l} - R_{\mu,l})^2\right] \tag{13}$$

where w_μ is the strength of the localizing potential in the direction of each main axis ($\mu = x,y,z$). We assume that the harmonic potentials are diagonalized in the same axes as the macroscopic strain. This is the simplest generalization of the isotropic model permitted by symmetry.

We find that, to obtain a result from this model, one must make a further assumption about the deformation of the tube variables $R_{\mu,p}$ with the applied strain. There are a range of possible assumptions, but generally the result depends on both the isotropic tube potential before the stretch, w_0, and the final w_μ.

If we make the particular assumption that the $R_{\mu,p}$ deform as

$$R_{\mu,p} = \lambda_\mu R_{0\mu,p}\left(\frac{1 + 3p^2/b^2w_\mu^{\,2}}{1 + 3p^2/b^2w_0^{\,2}}\right)^{1/2} \tag{14}$$

then the result obtained for the scattering function is independent of w_0.

$$N^{-2}\overline{\langle\rho_{\mathbf{q}}\rho_{-\mathbf{q}}\rangle_{\mathbf{R}}} = \int_0^1 \mathrm{d}x \int_0^1 \mathrm{d}x' \exp\left[-\sum_\mu Q_\mu^{\,2}\lambda_\mu^{\,2}\left|x-x'\right| + Q_\mu^{\,2}(1-\lambda_\mu^{\,2})\,\frac{d_\mu^{\,2}}{2\sqrt{6}R_\mathrm{g}^{\,2}}\left(1-\exp\left(-\frac{2\sqrt{6}R_\mathrm{g}^{\,2}|x-x'|}{d_\mu^{\,2}}\right)\right)\right] \tag{15}$$

where d_μ is related to w_μ in a manner analogous to eq 11. This result is very similar to the one used by Straube et al.[1] to fit their neutron scattering data, and it may be obtained by the substitution $d \rightarrow d_\mu$ in the original Warner–Edwards formula (eq 10). We emphasize, however, that this result depends on the assumption of eq 14 for the deformation of the tube variables $R_{\mu,p}$.

In the limit of a weakly cross-linked network dominated by entanglements, the form of coupling predicted by both Rubenstein and Panyukov[9] and Heinrich and Straube[10] is that the localizing potentials (due to topological interactions with neighboring chains) deform affinely with the strain:

$$w_\mu = w_0\lambda_\mu^{\,-1} \tag{16}$$

By analogy with eq 11, this gives a "tube diameter" which is anisotropic and couples to the strain nonaffinely, via

$$d_\mu^{\,2} = \lambda_\mu d_0^{\,2} \tag{17}$$

Physically, this "tube diameter" represents the mean-square fluctuation of a monomer about its mean position, and in this case the fluctuation is not isotropic. Straube et al. found that, if they coupled the tube potential to the macroscopic strain in this way, then eq 15 could fit their neutron scattering data along the major axes.[7] Unfortunately, the off-axis scattering was not well modeled, and a contour plot of eq 15 does not reproduce the lozenge shape.[1]

We also note that eq 15 does not give the experimentally observed isotropy angle. Within experimental error, it is found[1] that, for a specific angle between the scattering vector $\mathbf{q}$ and the stretch direction, the scattering is identical to that of the undeformed system. This angle is given by the condition

$$\sum_\mu q_\mu^{\,2}\lambda_\mu^{\,2} = \sum_\mu q_\mu^{\,2} \tag{18}$$

For the isotropy angle to be predicted by the above result (eq 15), direct substitution of eq 18 should yield the isotropic result,

$$N^{-2}\overline{\langle \rho_{\mathbf{q}}\rho_{-\mathbf{q}}\rangle_{\mathbf{R}}} = \int_0^1 \mathrm{d}x \int_0^1 \mathrm{d}x' \exp[-\sum_{\mu} Q_{\mu}^{\,2}|x - x'|] \qquad (19)$$

This holds only if the tube potential is isotropic; $d_x = d_y = d_z$. It is not possible to deform the tube potentials anisotropically while exactly retaining the isotropy angle. However, we will show later that the isotropy angle may be approximately reproduced while retaining a deformed tube potential.

Clearly, it is desirable to model the data for all wavevector directions, both along the major axes and off-axis, particularly with respect to the apparent isotropy angle. Within the bounds of the Warner–Edwards model, it is possible either to fit the data along the major axes (using deformed tube potentials, following Straube et al.) or to reproduce the isotropy angle (using isotropic tube potentials), but not to do both. We may conclude that, at the very least, some modification to the Warner–Edwards theory is necessary.

2.3. The use of Harmonic Potentials. The above results (eqs 10 and 15) both have the property of separability in the three main axes ($\mu = x,y,z$). This is a direct consequence of the use of harmonic localizing potentials for each monomer in the chain. The general form of the free energy for a harmonic localizing potential on monomer l is

$$F_l \sim (\mathbf{r}_l - \mathbf{R}_l)\cdot\mathbf{V}\cdot(\mathbf{r}_l - \mathbf{R}_l) \qquad (20)$$

and both our derivation and the original Warner–Edwards derivation[5] rely heavily on the form of this potential. The result would be different and much more difficult to obtain if a different form were used.

In order to reproduce the observed lozenges and isotropy angle, Straube et al. further modified eq 15 by replacing the tube diameter d_μ with a quantity d_ϕ which depended on the angle ϕ between the stretch axis and the scattering wavevector:[1]

$$d_\phi^{\,2} = \lambda_\phi d_0^{\,2}$$

$$\lambda_\phi^{\,2} = \lambda^2 \cos^2\phi + \lambda^{-1}\sin^2\phi \qquad (21)$$

The resulting expression was not separable in the main axes. Although this modification was based on physical arguments, the corresponding potential is not of the harmonic form (eq 20). Indeed, we do not believe that any form of localizing potential would give their expression. We must conclude that their modified expression is inconsistent with the original model.

2.4. Summary of Previous Theories. It is clear from the work of Straube et al. that the original Warner–Edwards expression is not sufficient to fit the observed neutron scattering curves. The question we must ask, then, is whether a modified version of the Warner–Edwards model can explain the data, and, if so, how much physical information can be derived from the consequent best fit of theory to experiment.

The modifications made by Straube et al.[1] involve three assumptions, each of which must be justified:

(1) The form of the coupling between the macroscopic strain and the harmonic localizing potentials. In keeping with the theory of Heinrich and Straube,[10] they use $d_\mu^{\,2} = \lambda_\mu d_0^{\,2}$.

(2) The deformation of the tube configuration with the strain. In using a result similar to eq 15, there is an implicit assumption that the positions of the localizing potentials deform according to eq 14.

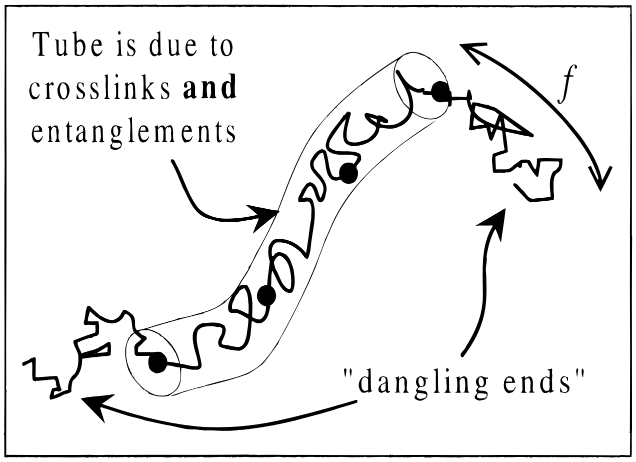

Figure 1. Schematic diagram of the "dangling ends" model.

(3) The assumption that the result can be modified so that it is nonseparable in the main axes. This was found to be necessary to obtain the lozenge pattern observed in the data contour plots.

One might argue that, given the apparent accuracy of their data fits, Straube et al. could be said to have successfully justified all three steps. However, we note that a full fit of their data required a modification (step 3 above) which was inconsistent with the original model. This raises two concerns. First, the fact that there was no derivation from a microscopic model means that parameters obtained from the fit cannot necessarily be related to any physical quantity. Second, the fact that the Warner–Edwards model does not seem to be able to reproduce the experimentally observed scattering patterns (i.e., the lozenge form) indicates that it may be missing some important features of the network.

Whether or not an anharmonic localizing potential could be used to reproduce the lozenge pattern is an open question, not to be addressed here. It is certain that the theory would not be straightforward.

Other calculations, making the approximations of phantom networks[13] or uniform density fields,[14] have given lozenge scattering patterns but have not been able to identify their physical origin. In the following section, we propose a simple physical mechanism for the appearance of lozenges.

3. A Mechanism for Lozenges

3.1. The "Dangling Ends" Model. We now demonstrate that the appearance of lozenges in neutron scattering patterns from deformed networks can be explained by the presence of material which remains undeformed by the strain. We illustrate this argument for pure networks with labeled chain paths by taking a simple model for the network chains.

Consider a pure network in which some of the chain paths are labeled. Each labeled chain is confined to its tube by cross-links and entanglements. However, as illustrated in Figure 1, the free ends of the chain can relax and become isotropic in the absence of excluded volume interactions. These "dangling ends" extend as far down the chain as the first cross-link, since entanglement constraints on this part of the chain may be relaxed by starlike breathing modes.[15] For this reason, the length of the dangling end may, in fact, be several tube diameters.

Calculation. For ease of calculation, we take the preaveraged model in which we assume that each chain in the system has two dangling ends of identical length, each a fraction f of the total length of the chain. Since all the averages involving the chain variables are Gaussian, the single-chain scattering function is of the form

$$S(\mathbf{q}) = \frac{1}{N^2}\sum_{l,l'}\exp[-G_q(l,l')] \tag{22}$$

where

$$G_q(l,l') = \frac{1}{2}\sum_\mu q_\mu^2\overline{\langle(r_{\mu,l} - r_{\mu,l'})^2\rangle} \tag{23}$$

and $\overline{\langle ... \rangle}$ represents an average over all quenched and annealed variables.

For the central chain segment confined to the tube, we take the Warner–Edwards model. For the sake of generality, we shall relax the constraint of isotropic tube potentials and allow a general tube diameter d_μ. We will show that lozenges are obtained independently of this constraint, but that exact reproduction of the isotropy angle requires isotropic tube potentials, $d_\mu = d_0$. Note, however, that we will use a solution which is separable in the main axes, as is required by Gaussian localizing potentials.

Although we could calculate eq 23 directly, this is unnecessary because we have effectively performed the calculation in deriving the Warner–Edwards result (eq 15). By comparison with eq 15, we find that, for any two monomers in the central tube section,

$$G_q(x,x') = \eta_q(x,x')$$

where

$$\eta_q(x,x') = \sum_\mu Q_\mu^2\lambda_\mu^2|x - x'| + Q_\mu^2(1 - \lambda_\mu^2)\frac{d_\mu^2}{2\sqrt{6}R_g^2}\left(1 - \exp\left(-\frac{2\sqrt{6}R_g^2|x - x'|}{d_\mu^2}\right)\right) \tag{24}$$

where we have used the contour length variables $x = l/N$ and $x' = l'/N$.

For the isotropic dangling ends, we take standard Gaussian chain statistics. For any two monomers in the same dangling end,

$$G_q(x,x') = \kappa_q(x,x')$$

where

$$\kappa_q(x,x') = \sum_\mu Q_\mu^2|x - x'| \tag{25}$$

Finally, we note that there is no correlation between the distributions of the dangling ends and the central tube segment. This means that, for monomer pairs in different chain sections, we can always split $G_q(x,x')$ into separate contributions from each chain section between the two monomers. Writing the sum over monomers in eq 22 as an integral, we find that the scattering function is

$$S(\mathbf{q}) = 2\int_0^1 dx\int_0^x dx' \exp[- G_q(x,x')] \tag{26}$$

where

$$G_q(x,x') = \begin{cases} \kappa_q(x,x') & \{x,x'\} \leq f \\ \kappa_q(f,x') + \eta_q(x,f) & f < x \leq 1 - f,\ x' \leq f \\ \kappa_q(f,x') + \eta_q(1 - f,f) + \kappa_q(x,\ 1 - f) & 1 - f < x,\ x' \leq f \\ \eta_q(x,x') & f < \{x,x'\} \leq 1 - f \\ \eta_q(1 - f,x') + \kappa_q(x,1 - f) & 1 - f < x,\ f < x' \leq 1 - f \\ \kappa_q(x,x') & 1 - f < \{x,x'\} \end{cases} \tag{27}$$

In the above calculation, we have apparently treated the dangling ends as completely isotropic. Nevertheless, it is an experimental fact (from NMR[16]) that dangling ends are stretched and at least partially oriented. This is due to the excluded volume couplings between stretched and isotropic portions of the chain.[17] However, in the special case where the deuterated and undeuterated chains are otherwise identical, eq 26 gives the correct behavior for the scattering intensity, which we expect to be of the form

$$I(\mathbf{q}) \approx \phi(1 - \phi)\, S(\mathbf{q}) \tag{28}$$

where ϕ is the fraction of deuterated chains. This result may be found in ref 18, and the scaling arguments presented there for the melt are applicable to the present system. We note that this result may also be derived directly from the random phase approximation (RPA) in the presence of quenched tube variables, though the calculation is lengthy and will be presented elsewhere.[19] Importantly, the structure factor $S(\mathbf{q})$ used in eq 28 should be the bare single-chain structure factor, calculated in the absence of excluded volume interactions and, thus, ignoring the orientation of the dangling ends. This is the structure factor we calculated above, and we note that it is an error to attempt inclusion of dangling end orientation directly in the single-chain structure factor.

The observation of dangling end orientation in NMR is certainly real and is not incompatible with the scattering formula (eq 28) given above. Indeed, a suitably chosen scattering experiment will also reveal the orientation. Suppose that, instead of labeling whole chains, the dangling ends alone were labeled. In this case, the scattering would be anisotropic, because the dangling ends are aligned by excluded volume interactions with stretched chain segments. On the basis of the resulting scattering pattern, we would rightly conclude that the dangling ends were oriented, and this would correlate with the NMR results. However, the converse is also true: if just the central, stretched portion of the chain were labeled, the same excluded volume interactions with the dangling ends result in a more isotropic scattering pattern than might otherwise be expected. Equation 28 applies only to an experiment in which whole chains are labeled. In this case, the total scattering from the dangling ends and the central chain portions gives the bare scattering function. The anisotropy due to alignment of the dangling ends is exactly canceled in the scattering pattern by the more isotropic central portions.

The above argument dispels the common misconception that the effects of dangling ends may be eliminated

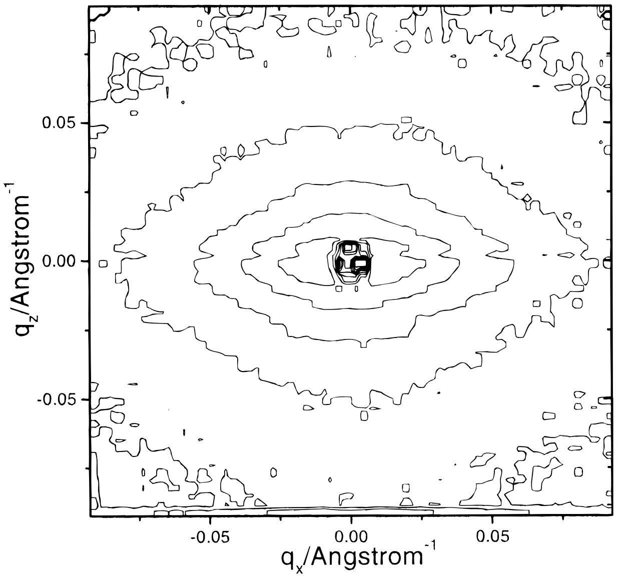

Figure 2. Contour plot of the two-dimensional scattering intensity from data obtained by Straube et al. on a stretched network ($\lambda = 2.9$) with labeled chain paths. The stretch is in the *z*-direction. Contours are for scattering intensities of (from the outside) 1.6, 3.3, 6.9, 14, and 30 in arbitrary units.

by labeling only the central portions of network chains. The dangling ends make their presence felt through the excluded volume interactions, and the effect is quite strong in the “incompressible” limit.

Equation 28 applies across the whole range of labeled chain concentrations, under the condition that the system is symmetric (the labeled chains are identical to the unlabeled ones). In the asymmetric case, one must resort to a more detailed RPA calculation,[19] taking full account of the excluded volume interactions and quenched tube variables. In general, we expect the result (eq 26) to hold in the limit of small concentrations of labeled chains, but the range of valid concentrations depends on the degree of asymmetry between the constituent chains.

Results and Discussion

Straube et al. have very kindly provided us with neutron scattering data from their experiment of ref 1. A contour plot of the two-dimensional scattering intensity for these data is shown in Figure 2, in which the characteristic lozenge shape is readily apparent. We have been able to obtain fits to these data using our formula (eq 26). For all the following results, we assumed their given experimental parameters of stretch ratio $\lambda_z = 2.9$ and a radius of gyration $R_g = 142$ Å for the labeled chains. We allowed for the possibility of tube potential deformation, via

$$d_\mu = d_0 \lambda_\mu^{\nu} \tag{29}$$

where the parameter ν was set either to $\nu = 0$ (isotropic tube potentials) or $\nu = {}^1/_2$ (deformed tube potentials, following Heinrich–Straube[10] and Panyukov–Rubenstein[9]).

Figure 3 shows a fit to the data at fixed $\nu = 0$ and $f = 0$ (i.e., for no dangling ends), the tube diameter d_0 being the fitting parameter. It is clear that the lozenge shape is not reproduced, and the theoretical contours are elliptical. For this reason, the fit is very poor. This fit corresponds to the basic Warner–Edwards model.

Figures 4 and 5 show contour plots at $\nu = 0$ and $\nu = {}^1/_2$ respectively, in which both the dangling end fraction f and tube diameter d_0 were allowed to vary to achieve the fit. Both curves reproduce the lozenge shape extremely well, though the fit for the deformed tube potential $\nu = {}^1/_2$ is marginally better (as measured by a sum of squares variable). The lozenge pattern can qualitatively be considered as a superposition of the isotropic scattering from the undeformed material and the elliptic scattering from the stretched chains, with correlations between the two accounted for.

We should point out that the dangling end fraction f required to fit the data is above 20% in both fits. Since the data given by Straube et al.[1] for the chain mass between cross-links suggest that, in their system, the dangling ends are 8% of the total chain length, we must state that the fitting value for f is unreasonably high. There are good reasons for this discrepancy. The method used to estimate f does not account for the sizeable quantity of chain scission which occurs during cross-linking and which increases the amount of “chain-

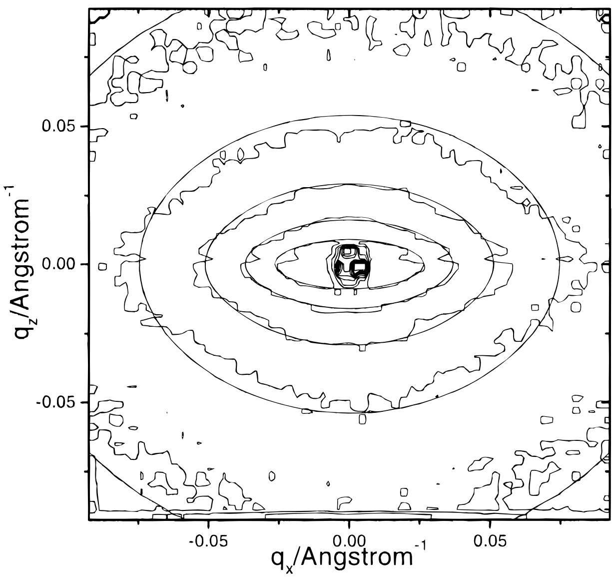

Figure 3. Fit to the data of Figure 2 using fixed $f = 0$, $\nu = 0$, $R_g = 142$ Å, $\lambda_z = 2.9$, $\lambda_x = \lambda_y = 0.587$. The fitting parameter was $d_0 = 82$ Å.

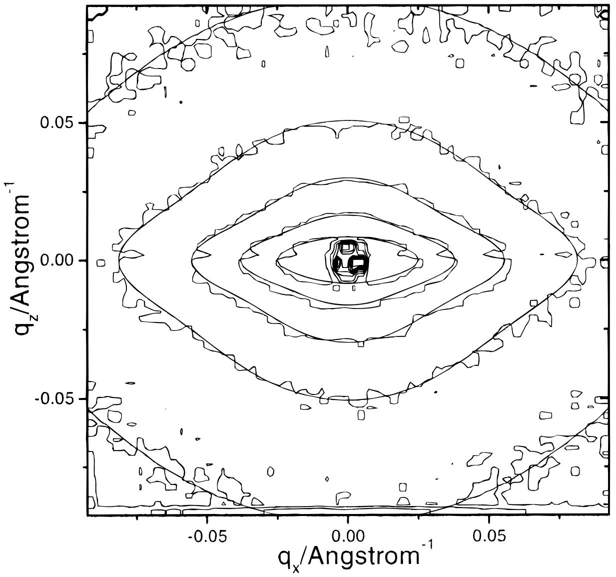

Figure 4. Fit to the data of Figure 2 using fixed $\nu = 0$, $R_g = 142$ Å, $\lambda_z = 2.9$, $\lambda_x = \lambda_y = 0.587$. The fitting parameters were $f = 0.23$ and $d_0 = 24$ Å.

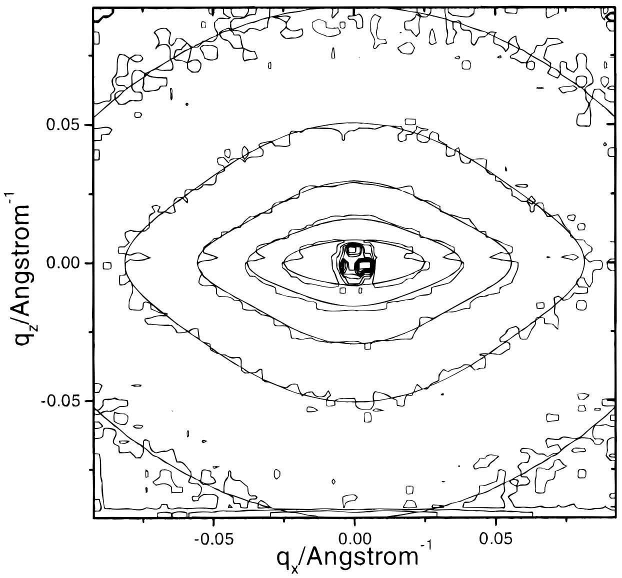

Figure 5. Fit to the data of Figure 2 using fixed $\nu = 1/2$, $R_g = 142$ Å, $\lambda_z = 2.9$, $\lambda_x = \lambda_y = 0.587$. The fitting parameters were $f = 0.21$ and $d_0 = 27$ Å.

end" material in the system. Also, in the Straube system, the unlabeled chains were not identical in size to the labeled chains, and so excluded volume interactions are not wholly accounted for. Finally, there will exist "loops" in the network, formed by chains cross-linking directly to themselves. While loops may be stretched via topological constraints with surrounding chains, it is to be expected that such stretching is much weaker than direct stretching via cross-links. By calculating the total number of chains within the typical volume occupied by a single-chain section between two cross-links, we estimate that the total chain fraction within loops may be as high as 5%.

A detailed model accounting for both chain scission during cross-linking and variations in chain size could only be treated using the full multicomponent random phase approximation. Such a calculation would need to include (i) chain scissions both before and after gelation, which are qualitatively different since chains broken after gelation remain localized while chains broken before gelation are free to explore the system volume, (ii) polydispersity, both in the overall chain size and in the dangling ends due to varied chain mass between cross-links, and (iii) excluded volume effects in the presence of quenched tube variables. We believe that points (i) and (ii) may prove prohibitive, although (iii) may be handled using theoretical tools recently developed by the present authors.[19] Furthermore, theoretical treatment of network loops is far from straightforward. Nevertheless, we suggest that the overall increase in unstretched material brought about by these effects may qualitatively be represented in our simple model by an increase in f. We are confident that a more detailed model would yield a more reasonable fitting parameter while retaining the quality of the fit.

The values for d_0 obtained in our fits (24 and 27 Å, respectively) may be compared with literature values for tube diameters in the same polymer (polyisoprene). From plateau modulus and neutron spin echo data in the melt, Richter et al.[20] obtain a tube diameter of $d_0 \approx 51$ Å. Since the cross-link separation in the network is of a similar order of magnitude to this (roughly 70 Å), we would certainly expect the network value for d_0 to be lower than that in the melt, because of the extra constraint due to cross-links. Furthermore, there are qualitative differences between the Warner–Edwards tube model for networks and the conventional tube model for melts, not the least of which is the fact that the chain is free to move along the tube in melts (such motion is suppressed by the localizing potentials in the Warner–Edwards tube). It is not obvious that melt tube diameters can be directly compared with those from networks. From stress-strain data in their networks, Straube et al.[1] quote a tube diameter of 37 ± 3 Å. However, it is not clear whether this calculation of the tube diameter allows for the presence of unstretched material in the network, which cannot contribute directly to the modulus. Inclusion of this effect should yield a lower value for the tube diameter, because the remaining, stretched chain must be more constrained to yield the same modulus. Given this, and the stated simplicity of our model, we are not unduly concerned by the apparent discrepancy.

The fact that the fit for $\nu = {}^1/_2$ is better than that for $\nu = 0$ is worthy of some discussion. In fact, we found that, in all comparable fits (for example, in all fits where f was fixed while varying d_0), fixing $\nu = {}^1/_2$ gave a better fit than $\nu = 0$. This seems to indicate that the best model for a real network does, in fact, involve coupling the tube potential to the strain, as has been suggested by Panyukov–Rubenstein[9] and Heinrich–Straube.[10] However, this evidence is, at best, suggestive since a good fit could be obtained using either value for ν.

Furthermore, coupling the tube potential to the strain in this way removes the exact prediction of an isotropy angle,[8] along which the scattering is identical to that of the undeformed network. Experimentally,[1] this angle is found to be given by the condition

$$\sum_\mu q_\mu^{\,2} \lambda_\mu^{\,2} = \sum_\mu q_\mu^{\,2} \tag{30}$$

Substituting this condition for $\hat{\mathbf{q}}$ into our eq 27, we find that

$$G_{\mathrm{q}}(x,x') = \sum_\mu Q_\mu^{\,2} |x - x'| \qquad \text{for all } \{x,x'\} \tag{31}$$

only under the condition $\nu = 0$. The isotropy angle is exactly reproduced only when the tube potential is isotropic, and this is illustrated in Figure 6, which is a contour plot of the difference $S(\mathbf{q},\lambda) - S(\mathbf{q},0)$ between the stretched and undeformed scattering functions for the fit to the Straube data with $\nu = 0$. The "zero contour" consists of two straight lines at a fixed angle to the stretch direction.

In Figure 7, we plot the equivalent contours of $S(\mathbf{q},\lambda) - S(\mathbf{q},0)$ for the fit with $\nu = {}^1/_2$. This does not exactly reproduce the isotropy angle, and the zero contour is not a straight line. However, it still lies close to the isotropy angle and is likely to be within experimental error.

Moreover, we note that, in order to obtain the isotropy angle experimentally, it is necessary to normalize the scattering from both the stretched and unstretched networks. This requires careful measurement of the quantity of material in the neutron beam and is subject to a certain degree of error. We might consider the effect on the zero contour of an error in the normalization. In Figure 8 we show a contour plot of $S(\mathbf{q},\lambda) - \alpha S(\mathbf{q},0)$ for the fit with $\nu = {}^1/_2$. We set $\alpha = 1.1$ to represent a cumulative error of 10% in the successive normalizations. It is clear from the theoretical curve

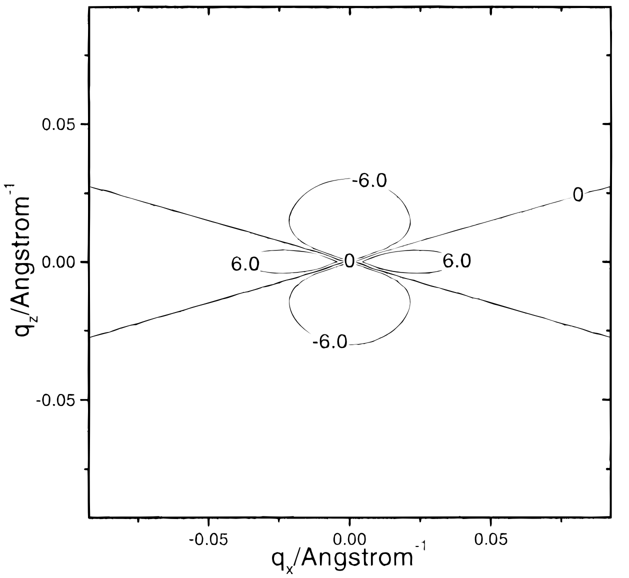

Figure 6. Contour plot of the difference $S(\mathbf{q},\lambda) - S(\mathbf{q},0)$ between the stretched and undeformed scattering functions for the same parameters as Figure 4.

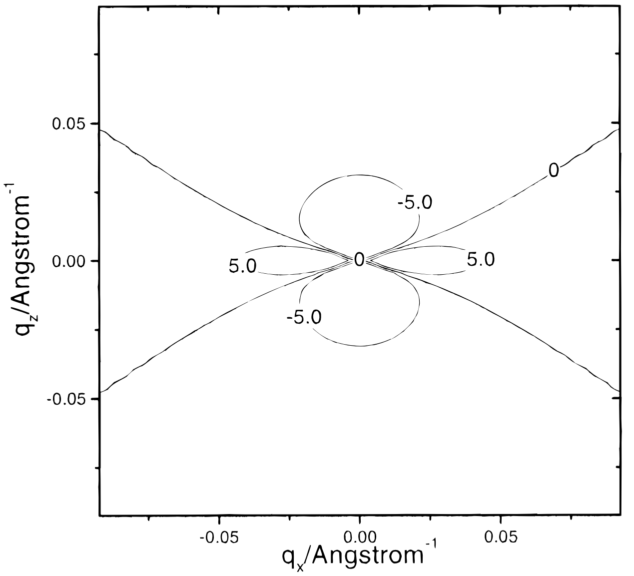

Figure 7. Contour plot of the difference $S(\mathbf{q},\lambda) - S(\mathbf{q},0)$ between the stretched and undeformed scattering functions for the same parameters as Figure 5.

that a “normalization error” has occurred, because the zero contour no longer passes through the origin, $\mathbf{q} = 0$. However, this would not be apparent in an experiment because the origin is masked by the beam stop. Outside the area of the beam stop, the zero contour is very nearly a straight line and lies extremely close to the isotropy angle, as defined in eq 30. This demonstrates that a deformed tube potential can easily result in the experimental illusion of an isotropy angle.

In the light of these results and in the absence of more precise experimental data, we should consider the isotropy angle to be an approximate rather than an exact result. We conclude that the isotropy angle does not provide sufficient evidence against a tube potential which couples to the strain. We also find that fits to lozenge-like scattering from the stretched network cannot distinguish sufficiently between isotropic and deformed tube potentials. The scattering experiments under discussion are, thus, not a good discriminator between proposed values of ν. Nevertheless, we do

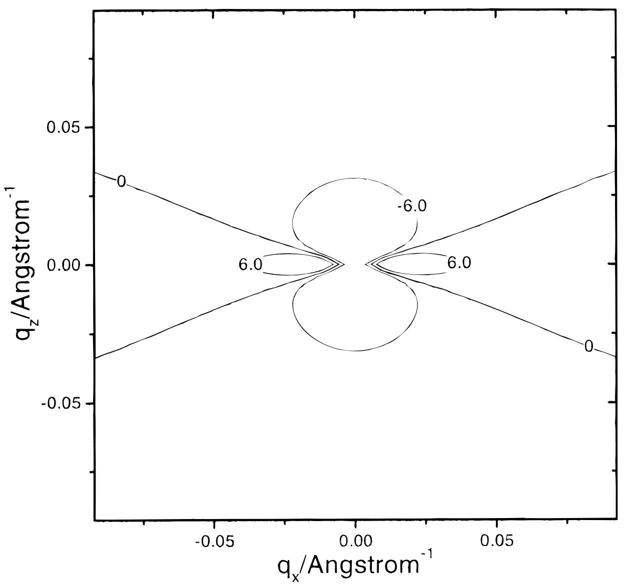

Figure 8. Contour plot of the incorrectly normalized difference $S(\mathbf{q},\lambda) - \alpha S(\mathbf{q},0)$ between the stretched and undeformed scattering functions for the same parameters as Figure 5, with $\alpha = 1.1$.

conclude that the lozenge shape can be quantitatively reproduced while retaining a physical microscopic model by accounting for dangling chain ends.

3.2. Connection with “Butterfly” Scattering Experiments.

For completeness, we now discuss the appearance of lozenges observed in the recent “butterfly” scattering experiments.[2,3] The butterfly is the name given to a contour plot where the contours have a characteristic “Figure-8” shape, aligned in the stretch direction. There are two commonly used systems which give butterflies: networks swollen by labeled mobile chains, and melts formed from a blend of long chains with shorter labeled chains. In the latter case, the long chains form a temporary entanglement network. In either case, it is generally accepted[3,21] that the appearance of the butterflies is related to static inhomogeneities in the density of network cross-links or entanglements. In the stretched system, the shorter mobile chains preferentially diffuse toward regions with fewer cross-links or entanglements because these regions are easier to swell. The deformation of the network is nonaffine, and the resulting anisotropic spacial distribution of the labeled chains gives rise to the butterfly contours.

The butterfly patterns do not appear immediately on stretching the system; there is typically a progression from elliptical contours to lozenges to butterflies. An explanation of the three shapes must take into account the time window in which each pattern is observed. In a recent experiment,[3] it was found that the ellipses appear when the system is first stretched, lozenges appear at times of the order of the orientational relaxation time for the short mobile chains, and butterflies appear at times a good deal greater than this (but less than the relaxation time of the long chains).

Clearly, the important time scale is the orientational relaxation time, τ_S, of the short chains. The ellipses correspond to the state where no chains have been able to relax and the system is affinely deformed. This can only be true at very short times, less than τ_S. At times of the order of τ_S, the short chains will have relaxed their orientation but will have had time to diffuse one radius of gyration at most. The equilibrium distribution of the short chains will be isotropic (though we can argue, as above, that excluded volume interactions with the network give them a degree of orientation). We propose that the combination of isotropic short chains and oriented long chains is sufficient to explain the lozenge shape in the scattering. The relevant calculation requires the introduction of excluded volume interactions between the stretched network and relaxed chains, while retaining affine network deformation and quenching the translational freedom of the chains. In fact, the uniform density field calculation of Edwards and McLeish[14] is equivalent to this, though it lacks physical interpretation and makes no connection with the butterfly patterns, nor any quantitative comparison with experiment. Nevertheless, we refer the reader who is interested in mathematical detail to ref 14.

At times much greater than τ_S, the short chains have had time to diffuse to regions of low network cross-link or entanglement density. This is the requirement for the onset of butterfly scattering patterns. The patterns eventually relax at the time scale of relaxation of the entanglement network.

4. Conclusion

In this paper, we have provided an explanation for the lozenge-shaped contour plots often observed in neutron scattering from stretched polymer systems. We have demonstrated that the presence of chain material which remains undeformed by the stretch is sufficient to give the lozenge patterns. The patterns can qualitatively be considered to be a superposition of isotropic and elliptic scattering functions. To illustrate this, we developed a model for network chains in which the central portion of the chain was confined to an Edwards tube, but in which the ends were free to relax. This model provided extremely good fits to the experimental data obtained by Straube et al. on partially labeled networks.

We investigated the possibility of coupling the localizing tube potential to the macroscopic strain in the manner proposed by Heinrich and Straube[10] and, more recently, Panyukov and Rubenstein.[9] We found that the experimental data could be fitted well by using either isotropic or deformed tube potentials. The fit using deformed tube potentials was marginally the better, but not conclusively so. We also pointed out that models using deformed tube potentials could only approximately reproduce the so-called “isotropy angle”, though the discrepancy is not sufficient to discount the deformed potential. We showed that an error in scattering normalization can easily create the illusion of an isotropy angle when none, in fact, exists.

Although the model was specifically designed for the case of scattering from pure networks with labeled chain paths, the concepts could easily be transferred to the case of lozenges which are precursors to butterfly scattering patterns in swollen gels. In these cases, we can qualitatively account for the evolution of the scattering with time.

There have been alternative explanations for the lozenge shape. We discounted the expression used by Straube et al. to fit their experimental data because, although it fitted the data well, it involved an inconsistent modification of the Warner−Edwards result. Their data fit cannot be related to any microscopic model.

A second possible explanation cannot be discounted so readily. It has been proposed[2,3,22] that the appearance of lozenges is due to a similar mechanism to the one which gives rise to butterfly scattering patterns. It is possible that the inhomogeneities in cross-link density give rise to nonaffine local deformations. This may result in an anisotropic scattering pattern, even in a pure network. In effect, this explanation is that the lozenge is, somehow, a superposition of elliptic and butterfly scattering patterns. We believe that this explanation arose historically because lozenges were often seen in experiments as a precursor to butterflies. Clearly, in these experiments it is impossible to neglect entirely the scattering effects due to the slight diffusion of chains at short times. It should be noted, however, that, in these butterfly patterns, the zero wavevector limit of the scattering is multivalued and depends on the direction of the scattering vector.[22,23] This does not appear to be a characteristic feature of the lozenge pattern. Furthermore, this model will not, in general, reproduce the isotropy angle observed in deformed pure networks.

In conclusion, we find that models involving a proper combination of isotropic and deformed chains will yield lozenge-like scattering patterns. This provides a reasonable and consistent explanation for the neutron scattering patterns observed in deformed polymer systems. Very careful control of the dangling end fraction will be required in SANS experiments which aim to discriminate between candidates for the tube potential coupling parameter, *v*.

Acknowledgment. D.J.R. gratefully acknowledges the financial support of ICI plc. We thank Straube et al. for kindly allowing us to use their data and W. Pyckhout-Hintzen for extremely useful discussions.

References and Notes

(1) Straube, E.; Urban, V.; Pyckhout-Hintzen, W.; Richter, D.; Glinka, C. J. *Phys. Rev. Lett.* **1995**, *74*, 4464−4467.
(2) Boué, F.; Bastide, J.; Buzier, M.; Lapp, A.; Herz, J.; Vilgis, T. A. *Colloid Polym. Sci.* **1991**, *269*, 195−216.
(3) Hayes, C.; Bokobza, L.; Boué, F.; Mendes, E.; Monnerie, L. *Macromolecules* **1996**, *29*, 5036−5041.
(4) See, e.g.: Deam, R. T.; Edwards, S. F. *Phil. Trans. R. Soc. A* **1976**, *280*, 317.
(5) Warner, M.; Edwards, S. F. *J. Phys. A* **1978**, *11*, 1649−1655.
(6) Westermann, S.; Urban, V.; Pyckhout-Hintzen, W.; Richter, D.; Straube, E. *Macromolecules* **1996**, *29*, 6165−6174.
(7) Straube, E.; Urban, V.; Pyckhout-Hintzen, W.; Richter, D. *Macromolecules* **1994**, *27*, 7681−7688.
(8) Boué, F. *Adv. Polym. Sci.* **1987**, *82*, 47.
(9) Panyukov, S. V.; Rubenstein, M. Preprint.
(10) Heinrich, G.; Straube, E. *Polym. Bull.* **1987**, *17*, 255.
(11) Read, D. J.; McLeish, T. C. B. *Phys. Rev. Lett.* **1997**, *79*, 87.
(12) Wagner, M. H. *Macromolecules* **1994**, *27*, 5223−5226.
(13) des Cloiseaux, J. *J. Phys. I (France)* **1993**, *4*, 539−550.
(14) Edwards, S. F.; McLeish, T. C. B. *J. Chem. Phys.* **1990**, *92*, 6855−6857.
(15) Ball, R. C.; McLeish, T. C. B. *Macromolecules* **1989**, *22*, 1911.
(16) McLoughlin, K.; Waldbeiser, J. K.; Cohen, C.; Duncan, T. M. *Macromolecules* **1997**, *30*, 1044−1052.
(17) Brereton, M. G.; Ries, M. E. *Macromolecules* **1996**, *29*, 2644.
(18) de Gennes, P. G. In *Scaling Concepts in Polymer Physics*; Cornell University Press: Ithaca, NY, 1979; pp 66−67.
(19) Read, D. J.; McLeish, T. C. B. To be published.
(20) Richter, D.; Butera, R.; Fetters, L. J.; Huang, J. S.; Farago, B.; Ewen, B. *Macromolecules* **1992**, *25*, 6156.
(21) Rouf, C.; Bastide, J.; Pujol, J.; Schosseler, F.; Munch, J. *Phys. Rev. Lett.* **1994**, *73*, 830−833.
(22) Panyukov, S. V. *JETP* **1992**, *75*, 347−352.
(23) Ramzi, A.; Zielinski, F.; Bastide, J.; Boué, F. *Macromolecules* **1995**, *28*, 3570.

MA970571K